Hindawi
International Journal of Chemical Engineering
Volume 2023, Article ID 2308227, 11 pages
https://doi.org/10.1155/2023/2308227

Review Article

The Production of Industrial-Grade Oxygen from Air by Pressure Swing Adsorption

Cynthia Chin,[1] Zykamilia Kamin ,[2] Mohd Hardyianto Vai Bahrun,[3] and Awang Bono[4]

[1]*WCT-CCCC Site Office, Jalan Sepangar Bay, Kota Kinabalu 88450, Sabah, Malaysia*
[2]*Oil and Gas Engineering Programme, Faculty of Engineering, Universiti Malaysia Sabah, Jalan UMS, Kota Kinabalu 88400, Sabah, Malaysia*
[3]*Department of Chemical Engineering, Faculty of Chemical and Energy Engineering, Universiti Teknologi Malaysia, UTM 81310, Johor Bahru, Johor, Malaysia*
[4]*GRISM Innovative Solutions, Kota Kinabalu, Sabah, Malaysia*

Correspondence should be addressed to Zykamilia Kamin; zykamilia@ums.edu.my

Received 19 August 2022; Revised 5 December 2022; Accepted 16 December 2022; Published 19 January 2023

Academic Editor: Witold Kwapiński

Copyright © 2023 Cynthia Chin et al. This is an open access article distributed under the Creative Commons Attribution License, which permits unrestricted use, distribution, and reproduction in any medium, provided the original work is properly cited.

Oxygen, an odorless and colorless gas constituent of the atmosphere, is a vital gas component for the Earth, as it makes up 21% of the composition of the air we breathe. Apart from the importance of oxygen for human breathing, its highly pure form is demanding for industrial applications. As such, several technologies have been established to increase the oxygen purity from 21% to somewhat higher than 95%. One of the competitive technologies for producing this high-purity oxygen from the air is through pressure swing adsorption (PSA), which has the advantages of low cost and energy while being highly efficient. Also, PSA is a simple and flexible system due to its ability to start up and shut down more rapidly since its operation occurs at ambient temperature, which is enabled through the use of adsorbents to bind and separate the air molecules. The enhancement of the PSA's performances was reported through the modification of PSA step cycles and material (zeolite) tailoring. A simplified complete set of a mathematical model is included for modelling the PSA system, aiming to ease the experimental burden of the process design and optimization of an infinite modification of PSA step cycles. Finally, some technological importance of oxygen production via PSA, particularly for onboard oxygen generation system and oxy-enriched incineration of municipal solid waste, was discussed. Continuous development of PSA will make significant contributions to a wide range of chemical industries in the near future, be it for oxygen production or other gas separation applications.

1. Introduction

High purity oxygen has received substantial attention as it is one of the essential industrial gases. According to the US CGA (compressed gas association), an oxygen-enriched air is a condition that comprises more than 21% composition of oxygen [1]. Industrial applications such as welding, medicine, combustion, refineries, and manufacturing metal require oxygen with more than 99% purity [2, 3]. Most particularly in the current emerging worldwide COVID-19 pandemic situation, whereby a rapid production of high-purity medical oxygen supplies for hospitals has been the key to treat COVID-19 patients [4, 5].

The production of oxygen can be accomplished either by cryogenic or noncryogenic methods. The cryogenic method was developed since the 1890s, by utilizing the principle of low-temperature distillation to separate the air constituents, which occurs at temperature around the boiling point of oxygen, i.e., at around −184°C [6]. Since oxygen has a lower boiling point than nitrogen (and argon), the oxygen is obtained in a top product stream. Conventionally, the gas undergoes liquefaction via the cryogenic distillation to produce a high-purity gas, through a series of cooling and compression stages. Due to this, it is an energy-intensive technology for providing compressions, expansions work, and cooling. As a result, it is highly expensive, and therefore,

suitable for high-tonnage quantities of the oxygen production. Additionally, a large amount of oxygen ($\geq 10^2$ TPD of oxygen) is the prerequisite for employing cryogenic air separation units [6].

To this end, the noncryogenic methods are developed, primarily to overcome the shortcomings of the erstwhile method, related to the issues of energy consumption and cost-competitiveness, especially when required at a smaller quantity [3]. Several technologies that are classified under the noncryogenic method include membrane separation and pressure swing adsorption (PSA). The membrane and PSA are relatively simple and economically feasible at moderate to low gas volumes. Furthermore, the noncryogenic method is more flexible for batch processing, with short start-up and shutdown times [7, 8]. Since the major factors restraining the growth of oxygen purification are technical and cost, the noncryogenic method is favourable in reducing energy consumption. At the same time, it improves its competitiveness against conventional technologies.

Considering the PSA technology for oxygen production, this technology has been introduced since 1960s by Charles Skarstrom through his patent [9]. Skarstrom pioneered the PSA processes in 1960, which is described as a "heatless" process since no separate heat source is required. The first PSA was used for air fractionation in the 1960s, while the early 1970s marked the commercial use of PSA for oxygen production [10, 11]. When it comes to adsorption, the solid material, termed as adsorbent, is the heart of the process, which greatly impacts the PSA separation performance. An adsorbent material must possess particular characteristics to be suited for applications in gas separation; in general, in terms of stability, regeneration, moisture resistance, cost, etc.

Reciprocating the invention of PSA, the researchers have attempted to develop models that can mathematically describe the underlying phenomenon of the process, be it rigorous complex or simplified modelling. The dynamic behaviour of PSA is the utmost important measure to determine its performance. Some of the studies on the modelling of PSA appear in Farooq et al. [12], Sakoda and Suzuki [13], Xu et al. [14], and Chang et al. [15]. The investigations primarily aimed for experimental verification checks so that the developed models are reliable for predicting the PSA behavior and performances.

This paper addresses the overview of the PSA process, highlighting its application in the production of industrial oxygen gas. The foundation of the PSA is first discussed with respect to the initial invention of the PSA by Skarstrom and some of its modifications on the addition of steps for enhancing the PSA performance. Then, the mathematical model is introduced as a theoretical framework for assessing the PSA system through a simplified complete set of equations. Then, the core of the adsorption process related to adsorbent materials that are typically used in oxygen production is highlighted with some modifications to them aiming for tailoring a better material. Also, the highlight of the discussion in the usage of the oxygen produced via PSA in two technological applications, i.e., on-board oxygen generation system (OBOGS) and oxy-enriched incineration municipal solid waste (MSW), is included. Finally, some knowledge gaps and future research in this field are presented.

2. The Configuration of the Pressure Swing Adsorption (PSA) Cycle

The breakthrough finding on gas separation using adsorption started since the invention of Skarstrom [9], which proposed a heatless adsorption separation process for air fractionation. The PSA process typically utilizes a two-bed column packed with solid adsorbent materials to produce oxygen; one column is in the adsorption state, while the other is in the desorption (regeneration) state. As the name suggested, the PSA exploits the variation of pressure to regenerate the adsorbent.

2.1. The Description of the Conventional Skarstrom Cycle. The conventional Skarstrom cycle, often referred to as the 2-bed, 4-step PSA cycle, operated in a cyclic manner, consists of the adsorption (AD), counter-current blowdown (BD), counter-current purge (PU), and concurrent pressurization [9]. The 4-step sequence of the conventional Skarstrom cycle is depicted in Figure 1.

The first step in the Skarstrom cycle is AD/PU, whereby the feed air mixture enters the first column at high pressure P_H, which contains an adsorbent material that selectively adsorbed a strongly adsorbable component from the air (N_2). The first column is said to be on the AD step. The outlet stream from the first column is obtained as a light product or oxygen-enriched gas at high purity. At the same time, the second column at a low pressure P_L is said to be undergoing a PU step by recycling a small fraction of light product discharged in the first column. The effluent drawn from the second column is obtained as a heavy product or lean gas (containing mixture of components—nitrogen-enriched gas).

The second step is the BD/PR. After the predetermined adsorption time is achieved, the second step starts, at which the first column will undergo a depressurization by releasing the pressure from the feed inlet. The first column is said to be undergone a counter-current blowdown. While the second bed undergoes cocurrent pressurization using the feed mixture after being purged in the first step. This step continues until both the first and second columns reach the predetermined desorption and adsorption pressure, respectively.

The third step is the PU/AD, which commences immediately after the second step. This step is similar to the first step, with the role of the bed being swapped. And the last step is the PR/BD, which is similar to the second step, with the role of the bed being swapped. Refer to Figure 1 to visualize the steps of the Skarstrom cycle.

In the Skarstrom cycle, a more strongly adsorbed component is generally separated and removed from the mixture of gases at high pressure, whereas desorption of the adsorbed component occurs at a lower pressure [9]. In oxygen production, a typical scenario is wherey oxygen

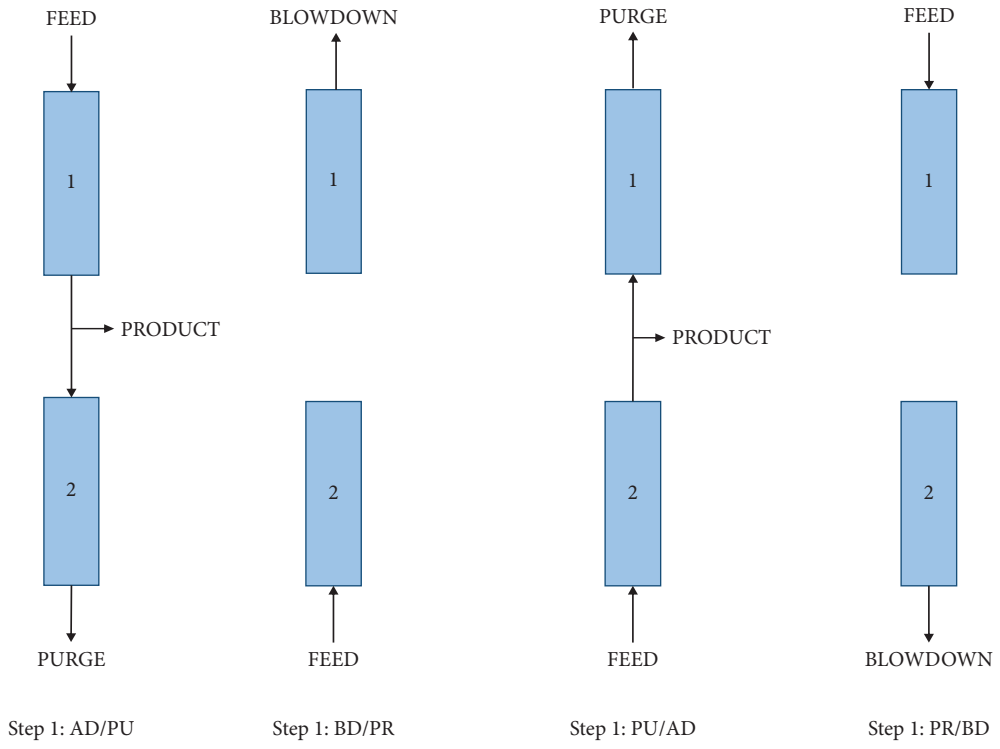

Figure 1: The typical two-bed, four-step Skarstrom cycle adapted from [16].

being a weakly adsorbed component than nitrogen; thus, nitrogen as the strongly adsorbed component is removed from the air [5].

2.2. The Advancement in the Variation of the PSA Cycle. Those previously mentioned steps and scenarios describe the four-step configuration of the Skarstrom cycle that was the initial invention of a PSA. Basically, the conventional Skarstrom cycle has a limitation in the recovery of a produced product, usually below 25% in a simple two-bed PSA [17]; thus, modifications of the cycle scheduling of the PSA cycle are often proposed to counter the limitation. Such variation in the PSA cycle includes the addition of pressure equalization and pressurization (with product). This section describes the said advancement of the PSA system, supported by art in patents and scientific articles.

2.2.1. Pressure Equalization Step. The pressure equalization (PE) in a PSA system was documented since the 1960s through patents Marsh et al. [18] and Berlin [19], with the objectives of improving the recovery of a strong adsorbable component and energy consumption associated with pressurizing-depressurizing. In practice, the PE step can be achieved by connecting the light product end of two beds—the high-pressure gas removed during the concurrent depressurization step to repressurize other beds by pressure equalization, which is referred to as a BB equalization. Or, tanks are utilized for equalization in between two beds, which is referred to as a BTB equalization. Several notable contributions to this improvement are from Hassan et al. [20], Yang [21], Jasra et al. [17], Ruthven et al. [22], and Chiang [23].

The effect of the number of BB PE steps on the performance of PSA can be referred to in the works by Doong [24], Shin [25], Yavary et al. [26], etc., that evaluate the effect of PE on product purity and recovery. Shin [25] showed that the incorporation of PE step into a 2-bed configuration increases the product purity (96.89–99.41%) and recovery (50.64–68.52%), as compared to the conventional Skarstrom. In addition, Doong [24] evaluated the effect of PE step on the specific product and yield, on predetermining the oxygen product purity of 94.5%. They found out that an overuse of PE step could contaminate the product and reduce the specific product, which indicates there are optimal conditions between specific product and yield. The recent work by Yavary et al. [26] demonstrated that a more PE step contributes to a higher product recovery but lowers the purity, suggesting a trade-off between both indicators. In fact, an earlier work by Banerjee et al. [27] proved that adding PE step could conserve energy through the recovery of mechanical energy contained in the high-pressure bed, and therefore reduce the cost of the technology.

The PSA cycle modification through pressure equalization step incorporating tank equalization has been proposed, as early as the invention of the Skarstrom cycle by Marsh et al. [18]. In the embodiment of their patent, they connected a tank for storing a fraction of enriched-gas product coming from the high-pressure bed and used it to purge the bed, after which the bed is subjected to purge with the product gas. By doing this, the consumption of purge product gas is reduced, thus

enhancing product recovery. As to accomplish for many tanks for BTB PE step, accurate modelling is required for the design. To this end, many researchers have attempted for accurate modelling of BTB PE step, since the incorporation of the empty tank could lead to the disruption of the material balance of the overall system, and thus, its inaccuracy could lead to a notable effect on the PSA performance [28, 29].

2.2.2. Pressurization (with Product) Step. A common practice of the conventional Skarstrom cycle utilizes a pressurization step using the feed mixture to raise the bed's pressure to the adsorption pressure, P_H. A novel approach, as opposed to the prior practice, is by pressurizing the adsorbent bed using a product stream [30], using either the enriched or the lean product gas.

Knaebel and Hill [16] compared both pressurization step practices (using feed and product) toward the product recovery using an equilibrium theory. They found out that the latter gives a higher product recovery, to the extent of the product recovery improvement becoming better for small separation factors, small fractions of the light component (O_2) in the feed, and large pressure ratio, P_H/P_L. Later, their findings were verified experimentally by Kayser and Knaebel [31]. To be clear, the pressurization step studied by Knaebel and coworkers uses an enriched product gas.

In addition, Vo [32] proposed a slightly different view in using the product gas for the pressurization step, which is using a lean product gas (below 5% offset than the predetermined purity of the lean gas) and slightly different sequential steps of the PSA cycle. In the patent embodiment, it claimed that an enriched product gas could be achieved in the range of 90–99% purity.

3. Mathematical Model of PSA

In the last few decades, pressure swing adsorption (PSA) has become increasingly popular as a technology for producing oxygen from the air. Efforts at modelling and simulating the PSA cycles have been aimed to reduce the experimental burden for process design and optimization; as such, the modelling of PSA is capable at predicting the concentration, temperature and pressure profiles, and cycle performance parameters. The material, momentum, and energy balances must be considered to model a rigorous PSA process. Several model assumptions were used as a foundation of building the model [33]. These include

(1) The bulk gas phase is considered an ideal gas, PV = nRT

(2) The bed properties, such as porosity and bulk solid density, is assumed to be uniform in both axial and radial coordinates

(3) No reaction was involved between the adsorbed gas and solid adsorbent

(4) The radial temperature and concentration gradients are insignificant.

(5) The adsorption rate is approximated by a linear driving force (LDF) model.

3.1. Material Balance. Based on the assumptions made above, the equation used for the one-dimensional is shown in equation (1). The equation shows that the net change in the gas phase and adsorbed phase within the packed bed column is equivalent to the net flow of the bed [34].

$$\varepsilon_t \frac{\partial c_i}{\partial t} + \rho_b \frac{\partial q_i}{\partial t} - D_{ax,i} \frac{\partial^2 c_i}{\partial z^2} + \frac{\partial v_g c_i}{\partial z} = 0. \quad (1)$$

3.1.1. Mass Transfer Rate. In most of the adsorption modelling analyses, a linear driving force (LDF) approximation is often implemented for describing the transference of the adsorbate from the bulk fluid phase to the solid adsorbent phase. The LDF model can be described as a function of the solid or fluid film difference of the adsorbate component. The following equation expresses the LDF model as a function of the solid film difference [35]:

$$\frac{\partial q_i}{\partial t} = k_{LDF}\left(q_i^* - q_i\right). \quad (2)$$

The q_i^* is obtained through the relation of the fluid-solid equilibrium at constant temperature, which is expressed as an adsorption isotherm.

3.1.2. Equilibrium Adsorption Isotherm Relations. The adsorption of gas molecules onto the surfaces of the solid adsorbent is governed by a mathematical expression that measures the extent of the adsorption in an adsorbate/adsorbent system, which is known as equilibrium adsorption isotherm when it is measured at varying pressure with a constant temperature [33]. Many adsorption isotherms have been applied to describe the equilibrium relationship between the gas and adsorbed phases as a function of pressure; among others are Langmuir, Freundlich, Langmuir–Freundlich, etc. As the original isotherm equations (Langmuir, Freundlich, Langmuir–Freundlich, etc.) are based on a single component, an extended version of each is used to accurately describe the multicomponent effect toward the system. It is observed from the literature that the extended Langmuir (equation (3)) and extended Langmuir–Freundlich (equation (4)) isotherms for binary N_2/O_2 mixture are the most widely best-fitted model for this purpose.

(a) Extended Langmuir isotherm:

$$q_i^* = \frac{q_{m,i} K_{L,i} P_i^*}{1 + \sum_{j=1}^{N} \left(K_{L,j} P_j^*\right)}, \quad (3)$$

where $q_{m,i} = k_i + k_2 T$ and $K_{L,i} = k_3 e^{k_4/T}$.

(b) Extended Langmuir–Freundlich isotherm:

$$q_i^* = \frac{q_{m,i} K_{L,i} P_i^*}{1 + \sum_{j=1}^{N} \left(K_{L,j} P_j^*\right)}, \quad (4)$$

where $q_{m,i} = k_i + k_2 T, K_{L,i} = k_3 e^{k_4/T}$ and $n_i = k_5 + k_6/T$.

The related literature on the adsorption isotherm for the extended Langmuir and extended Langmuir–Freundlich model is summarized in Table 1, consisting of various adsorbents from the zeolites family.

In case of only measurement on a pure single component isotherm is available, the solution theories (ideal adsorbed or vacancy) are often employed to account for the multicomponent effect and generally provide reasonable and reliable accuracy with the multicomponent experimental results [41–43]. The ideal adsorbed solution theory (IAST) and vacancy solution theory (VST) descriptions can be found in ref. [22, 44] that provide a thorough discussion of both theories on the multicomponent adsorption system.

3.2. Momentum Balance. When considering the pressure drop across the bed, several models can be used to describe the momentum balance, such as Darcy's, Ergun's, Karman–Kozeny's, and Burke–Plummer's equations. Their respective equations are expressed in equations (5)–(7) , respectively, as listed in Table 2.

It is worth noting that the Darcy equation is suitable to be used when the Reynolds number, $\mathrm{Re} < 10$ [45], while the Ergun equation, which excludes the effect of the surface roughness, is best used when $\mathrm{Re} > 10$. Meanwhile, the Karman–Kozeny equation is valid for evaluating pressure drop in an adsorption bed with a laminar flow with $\mathrm{Re} \leq 10$, whereas the Burke–Plummer equation is applied for turbulent flow with $\mathrm{Re} \geq 1000$, which represents kinetic losses [46].

3.3. Energy Balance. The nonisothermal process of PSA is contributed by the heat adsorbed and released throughout the cycle, which is governed by various aspects, including heat of adsorption, heat convection and conduction, and thermal accumulation [33]. A complete energy balance equations require three control volumes to be defined, which are gas-phase, solid-phase, and wall. Equations (5)–(7) express the abovementioned control volumes' energy balance, respectively [34].

$$-k_{ga}\varepsilon_i \frac{\partial^2 T_g}{\partial z^2} + C_{vg}\nu_g \rho_g \frac{\partial T_g}{\partial z} + \varepsilon_t C_{vg} \rho_g \frac{\partial T_g}{\partial t} + P\frac{\partial \nu_g}{\partial z} + HTCa_p\left(T_g - T_s\right) + \frac{4H_w}{D_B}\left(T_g - T_o\right) = 0, \quad (5)$$

$$-k_{sa}\frac{\partial^2 T_s}{\partial z^2} - \rho_s C_{ps}\frac{\partial T_s}{\partial t} + \rho_s \sum_{i=1}^{n}\left(C_{pai} q_i\right)\frac{\partial T_s}{\partial t} + \rho_s \sum_{i=1}^{n}\left(\Delta H_i \frac{\partial q_i}{\partial t}\right) - HTCa_p\left(T_g - T_s\right) = 0, \quad (6)$$

$$-k_w \frac{\partial^2 T_w}{\partial z^2} + \rho_w c_{pw}\frac{\partial T_w}{\partial t} - H_w \frac{4D_B}{\left(D_B + W_T\right)^2 - D_B{}^2}\left(T_g - T_w\right) + H_{amb}\frac{4\left(D_B + W_T\right)^2}{\left(D_B + W_T\right)^2 - D_B{}^2}\left(T_w - T_{amb}\right) = 0. \quad (7)$$

To complete and solve the governed mathematical model (mass, momentum, and energy), some model parameters that are unknown can be estimated using reliable correlations with reasonable accuracy to the overall performance of the PSA system. A short review paper by Kamin et al. [5] summarises related correlations for estimating the unknown model parameters. The comprehensive list of established correlations can be found in many separation processes and mass and heat transfer books [47, 48].

4. Adsorbents for PSA Oxygen Production

In PSA, two columns (a typical configuration) are packed with adsorbents, particularly a nitrogen-selective adsorbent for producing oxygen. Basically, the adsorbent that exhibits a higher microporosity is being used in the PSA as this class of adsorbent plays a vital role in the adsorption process, as such it provides more surface area for the favourably adsorbed species to be retained during the adsorption process. A promising adsorbent should have a high adsorption capacity and selectivity and can be regenerated.

4.1. Zeolite Molecular Sieves. The most common adsorbents used in air separation for producing oxygen come from the zeolites family. Zeolite is preferred for N_2 adsorption due to its higher selectivity towards it, thus making it suitable for oxygen production. Other unique features of zeolites that make them suitable for gas separation, in general, include high thermal and hydrothermal stability, uniform pore structure, easy pore aperture modification, and high adsorption capacity at a wide range of pressure [17]. The general formula of zeolite can be written as $M_{2/n}O...Al_2O_3...xSiO_3...yH_2O$, where M is any alkali or alkaline Earth atom, n is the charge on the atom, x is the ratio of silica and alumina (varies between 2 and 10), and y is stoichiometrically ranging from 2 to 7 [49].

The extra framework cation is the characteristic of zeolite that contributes to the preferential adsorption from nitrogen to oxygen [37] because there is a strong interaction between the quadruple moment of nitrogen with the cations of the zeolite framework, since it is approximately four times than that of oxygen. Among the zeolites, the zeolites 5A and 13X, being the nitrogen-selective zeolites, are the most commonly

Table 1: The adsorption isotherms' parameters of various zeolites for O_2/N_2 separation fitted using extended Langmuir and extended Langmuir–Freundlich model.

Adsorbents	Gas component		References
	O_2	N_2	
Extended Langmuir			
*LiX	$k_1 = 7.87 \times 10^{-9}$ mol/kg/Pa $k_2 = 1541.211$ K $k_3 = 6.79 \times 10^{-10}$ 1/Pa $k_4 = 1968.24$ K	$k_1 = 9.86 \times 10^{-9}$ mol/kg/Pa $k_2 = 2010.908$ K $k_3 = 1.67 \times 10^{-10}$ 1/Pa $k_4 = 2250$ K	Yang et al. [36]
$Li_{94.5}Na_{1.5}$-X	$k_1 = 1.14 \times 10^{-6}$ mol/kg $k_2 = 239.2$ K $k_3 = 2.20 \times 10^{-3}$ 1/atm $k_4 = 1092$ K	$k_1 = 1.69 \times 10^{-6}$ mol/kg $k_2 = 134.4$ K $k_3 = 1.19 \times 10^{-3}$ 1/atm $k_4 = 1990$ K	Hutson et al. [37]
$Li_{94.2}Na_{0.7}Ag_{1.1}$-X	$k_1 = 0.965 \times 10^{-6}$ mol/kg $k_2 = 196$ K $k_3 = 2.25 \times 10^{-3}$ 1/atm $k_4 = 1212$ K	$k_1 = 2.12 \times 10^{-6}$ mol/kg $k_2 = 64.82$ K $k_3 = 7.78 \times 10^{-3}$ 1/atm $k_4 = 1494$ K	
Extended Langmuir–Freundlich			
13X	$k_1 = 6.705 \times 10^{-3}$ mol/g $k_2 = -1.435 \times 10^{-5}$ mol/g/K $k_3 = 3.253 \times 10^{-4}$ 1/atm $k_4 = 1428$ K $k_5 = -0.3169$ $k_6 = 387.8$ K	$k_1 = 12.52 \times 10^{-3}$ mol/g $k_2 = -1.785 \times 10^{-5}$ mol/g/K $k_3 = 2.154 \times 10^{-4}$ 1/atm $k_4 = 2333$ K $k_5 = 1.666$ $k_6 = -245.2$ K	Jee et al. [38]
5A	$k_1 = 7.252 \times 10^{-3}$ mol/g $k_2 = -1.820 \times 10^{-5}$ mol/g/K $k_3 = 54.19 \times 10^{-4}$ 1/atm $k_4 = 662.6$ K $k_5 = -1.101$ $k_6 = 656.4$ K	$k_1 = 6.21 \times 10^{-3}$ mol/g $k_2 = -1.27 \times 10^{-5}$ mol/g/K $k_3 = 1.986 \times 10^{-4}$ 1/atm $k_4 = 1970$ K $k_5 = 2.266$ $k_6 = -396.5$ K	Jee et al. [39]
Li-LSX	$k_1 = 0.4789 \times 10^{-3}$ mol/g $k_2 = 636.6$ K $k_3 = 94.8 \times 10^{-4}$ 1/atm $k_4 = 500$ K $k_5 = 1.08168$	$k_1 = 1.84559 \times 10^{-3}$ mol/g $k_2 = 139.68$ K $k_3 = 2.19 \times 10^{-4}$ 1/atm $k_4 = 2484.2$ K $k_5 = 1.033$	Epiepang et al. [40]
Ca-LSX	$k_1 = 0.01448 \times 10^{-3}$ mol/g $k_2 = 1385.97$ K $k_3 = 1278.8 \times 10^{-4}$ 1/atm $k_4 = 207.35$ K $k_5 = 1.152$	$k_1 = 0.2623 \times 10^{-3}$ mol/g $k_2 = 646.75$ K $k_3 = 0.688 \times 10^{-4}$ 1/atm $k_4 = 3785.11$ K $k_5 = 0.931$	
$Li_{2.5}Ca_{46.75}$-LSX	$k_1 = 1.89933 \times 10^{-3}$ mol/g $k_2 = 145.55$ K $k_3 = 6.20294 \times 10^{-4}$ 1/atm $k_4 = 1609.13$ K $k_5 = 1.021$	$k_1 = 1.31846 \times 10^{-3}$ mol/g $k_2 = 104.23$ K $k_3 = 0.19726 \times 10^{-4}$ 1/atm $k_4 = 3489.63$ K $k_5 = 0.958$	
$Li_{4.2}Ca_{45.9}$-LSX	$k_1 = 2.20255 \times 10^{-3}$ mol/g $k_2 = 179.35$ K $k_3 = 4.02105 \times 10^{-4}$ 1/atm $k_4 = 1525.38$ K $k_5 = 0.992$	$k_1 = 0.98863 \times 10^{-3}$ mol/g $k_2 = 149.34$ K $k_3 = 0.467445 \times 10^{-4}$ 1/atm $k_4 = 3243.35$ K $k_5 = 0.999$	

*The expression of the extended Langmuir is slightly different. This may refer to the original work cited.

used in oxygen production. The zeolite 5A has a smaller pore size than zeolite 13X (5 Å versus 9 Å), which attribute to the significant adsorption performance of zeolite 5A through a low mass transfer resistance within the adsorbent [50]. Nowadays, the best commercial zeolite used in the oxygen production is a lithium-exchangedlow-silica zeolite, LiLSX, owing to the presence of Li^+ that increases the N_2 capacity (minimum 70% Li, near 100% Li is better). In contrast, it decreases the O_2 capacity due to the polarizability of Li^+ being lower than Na^+. This effect can be explained through the locality of Li cations. Since Li cation is mobile and smaller than Na cation, it can sit crystallographically very low in the six-ring that are not fully exposed to the supercage where N_2 and O_2 are located. This breakthrough invention of LiLSX has resulted in experiencing a cost reduction in oxygen production using LiLSX-loaded PSA [51].

Table 2: Several pressure drop models that are widely adapted for different flow conditions [34].

Model	Equation	Equation no
Darcy equation	$\partial P/\partial z = -K_P v_g$	Equation (5)
Ergun equation	$\partial P/\partial z = -[(1.50 \times 10^{-3}\mu(1-\varepsilon_i)^2 v_g)/(\varepsilon_i^3 (2r_p\ \psi)^2) + (1.75 \times 10^{-5}(1-\varepsilon_i)M\rho_g v_g^2)/(2r_p\psi\varepsilon_i^3)]$	Equation (6)
Karman–Kozeny equation	$\partial P/\partial z = -[(1.50 \times 10^{-3}\mu(1-\varepsilon_i)^2 v_g)/(\varepsilon_i^3 (2r_p\psi)^2)]$	Equation (7)
Burke–Plummer equation	$\partial P/\partial z = -[(1.75 \times 10^{-5}(1-\varepsilon_i)M\rho_g v_g^2)/(2r_p\psi\varepsilon_i^3)]$	Equation (8)

4.2. Modifications of Zeolite Molecular Sieves. Lately, great attention has been given to tailoring the zeolite adsorbents with high adsorption capacity for N_2. At the heart of this concept, Si/Al ratio modification and mixed cation are introduced. This section will describe the modifications used to improve the N_2 adsorption on zeolites.

4.2.1. Si/Al Ratio. Generally, the zeolite materials can be classified based on the Si/Al ratio: low silica (Si/Al ≤ 2), intermediate silica (2 < Si/Al ≤ 5), and high silica (Si/Al > 5) [52]. Generally, a lower Si/Al ratio is preferable since it increases the cation content because more Al atoms are substituted into the framework, thus enhancing the adsorption ability [53]. For example, Moradi et al. [54] investigated the effect of Si/Al ratio in a faujasite structure on the adsorption of CH_4. They observed an improvement in the CH_4 adsorption capacity when the Si/Al ratio was reduced from 3 to 1. A similar finding was observed by Chen et al. [53] on the adsorption of CO_2 onto FAU zeolites, in which they investigated the range of Si/Al ratio from 31 to 1. Talesh et al. [55] also reached similar outcomes on the adsorption of CO_2.

The underlying reasons behind the enhancement of the improved adsorption capacity at a lower Si/Al ratio are particularly due to more Lewis acid sites in the framework as the amount of Al increased [53]. This increases the surface cationic density and heterogeneity, which promotes the adsorption of a stronger quadrupolar molecule [55]; in the case of N_2/O_2 separation, the quadrupole moment of N_2 is four times stronger than O_2. In addition, the improved adsorption capacity can also be related, to a lesser extent, to increase the BET specific surface area at a lower Si/Al ratio [56, 57].

4.2.2. Mixed Cations. The exploration of mixed cations zeolites has also proven to enhance the adsorbability of zeolites toward the gas components, most particularly mixed with silver, as silver is known to have very strong effects on the adsorption characteristics of zeolites [37].

Hutson et al. [37] modified the LiX zeolite by incorporating a silver cation into its framework to demonstrate a mixed cation (Li^+ and Ag^+). They added Ag onto the LiX framework, and under appropriate dehydration conditions, the adsorptive characteristics of the newly formed mixed cation zeolites slightly increased in the capacity to adsorb N_2, resulting in a substantially improved product throughput (>10% increment) at the same product purity and recovery (from the PSA simulation). Combining the LiX zeolite with Ag^+ has been proven to enhance the adsorption capacity and thus, the PSA performance.

Recently, Epiepang et al. [58] investigated the mixed cation containing Li and Ca onto Sr-LSX and Ca-LSX zeolites for air separation, particularly N_2 adsorption. Among the mixed-cation (LiSr-LSX, AgCa-LSX, and AgSr-LSX) zeolite, AgCa-LSX zeolite displays an improved performance towards N_2 capacity, higher than Li-LSX at the studied temperature (298, 323, and 343 K). At the same time, the O_2 capacity increased, thus lowering the working capacity of AgCa-LSX, resulting in a detrimental effect on the O_2 productivity when performed in the PSA/VPSA setting. Though the mixed-cation in their study enhanced the performance compared to their single-cation precursors, the well-established zeolite Li-LSX still demonstrated superior performance for the oxygen production application.

The contributing mechanism behind the improvement of the adsorptive capacity of the mixed cation zeolites (relative to their single cation) can be attributed by the location optimality at which the cations sit in the zeolite frameworks. This is particularly important through the shielding effect of electrostatic energy of the cation and preventing interaction with adsorbates. Through molecular orbital calculations, the N_2 adsorption was enhanced by weak chemical interaction with the Ag^+ cation (in the case of silver mixed cation) on the zeolite framework [59].

5. Technological Processes Using PSA for Oxygen Production

This section presents the usage of the PSA in producing oxygen in the on-board oxygen generation system (OBOGS) and oxy-enriched incineration municipal solid waste (MSW).

5.1. On-Board Oxygen Generation System (OBOGS). The on-board oxygen generation system has become a principal technology for producing breathable oxygen on-board military aircraft, replacing bottled liquid oxygen, and providing pilots with an unlimited source of oxygen-enriched breathable air. The primary feed in the OBOGS for producing oxygen in military aircraft comes from engine bleed air [60]. The OBOGS offers several merits, including reduced life cycle cost, lessened logistic support, increased aircraft versatility, and most importantly, improved safety [61].

Beaman [62] developed a complete OBOGS PSA process model consisting of two zeolite-packed molecular sieves for the generation of aircraft crew breathing requirements. The system model developed includes the zeolite beds, rotary valve, purge orifice, and plenum breathing chamber and capable of favourably agreeing with the experimental results. As the PSA was still unable to surpass the standard of a liquid oxygen generator in that era, the works by Miller and coworkers [61, 63] explored a layered 2-bed PSA cycle (total of four bed sections, each of two was stacked) for producing high-purity oxygen for oxygen generation system, aiming for replacing the liquid oxygen system (LOX) that is

currently employed in the military aircraft. The small-scaled experimental tests achieved oxygen purity up to 99.7%, using a layered bed consisting of zeolite molecular sieve and carbon molecular sieve.

The innovation of OBOGS for military aircraft is never-ending, whereby the recent study conducted by Bhat et al. [60] evaluated the OBOGS using Li-LSX molecular sieve at different inlet pressures, product flowrates, and altitudes. Their laboratory tests of their OBOGS conform to the requirements specified by the military specification: concentrator oxygen (MIL-C-85521 (AS)) to be used in military aircraft. The most recent work related to OBOGS was carried out by Guo et al. [64] related to the development of a control scheme for a multistage oxygen noncrank compressor unit. Their findings showed that the motion control scheme gives excellent accuracy, with an error of less than 2%, with a stable discharge pressure and temperature. The great ability of the control scheme demonstrated for the noncrank compressor unit could potentially replace the conventional crank compressor that is currently employed in the OBOGS.

5.2. Oxy-Enriched Incineration of Municipal Solid Waste (MSW). Municipal solid waste (MSW) refers to trash for disposals, such as food residue, clothing, newspapers, and wood waste. One of the most effective ways of handling the ever-increasing MSW is incineration owing to its benefits of significant volume reduction (~90% volume reduction from the initial MSW) and energy recovery [65]. However, the conventional way of MSW incineration is associated with several disadvantages, including flue gas emissions, contaminated fly ash, and combustion instability [66].

The oxy-enriched combustion or incineration (OEC) of MSW appears capable of addressing the conventional incineration issues, through the use of O_2/N_2 as an oxidizing agent with an oxygen concentration higher than 21% (typically lesser than 30%). The uses of OEC have several merits, such as high combustion efficiency, low pollutant emissions (CO_2 concentration of only 30–40 vol%), acceleration of combustion speed, and promotion of combustion safety [67–69].

Currently, the oxygen supply for OEC in MSW typically comes from the cryogenic distillation and PSA technologies. In the view of producing the oxygen gaseous, the usage of PSA has a great potential for supplying higher oxygen purity for the OEC in MSW incineration, directly in gaseous form and the proven feasibility of the PSA in treating a low to medium capacity in terms of cost and simplicity, as such the oxy-enriched incineration furnace of MSW typically requires the oxygen of less than 100 ton/day [70]. Despite the higher installation (capital) cost of integrating PSA in the OEC, the cost associated with PSA oxygen generators will be stable for an extended period and may even decrease as its development becomes more sophisticated [70].

6. Knowledge Gaps and Future Research

Based on the current review of oxygen production from atmospheric air using pressure swing adsorption, several knowledge gaps have been identified, which may lead to more possibilities for future research in this field.

It has been noticed that oxygen production using PSA always utilizes a zeolite adsorbent, which is a nitrogen-selective adsorbent. Since air has a lower composition of oxygen than nitrogen, an oxygen-selective adsorbent is theoretically a promising choice since a small amount of adsorbent will be required, thus tailoring an oxygen-selective adsorbent for this purpose is one of the promising future research in this field. As such, the conventional Skarstrom cycle is becoming inappropriate to be used for the previously mentioned adsorbent's type; hence, an advanced configuration that is the enriching reflux cycle is required. The research area on the metal-organic framework (MOF)-based materials is the current direction in material science and engineering and should be explored to be used for adsorbent in oxygen production using PSA.

Lastly, there is a lack of review on the art in patent literature regarding the innovation of PSA for gas separation, particularly for oxygen production. Though this current review did some inclusion of patent literature; however, the vast amount of patents publicly available is not being used well. This could lead to uncertainty in some aspects of the patent as it is not perfectly understood. Hence, a review focusing only on the patent literature is critical.

7. Conclusion

The necessity of producing industrial-grade oxygen has led to the advancement of many technologies, which have low energy penalties, cost-competitive, and easy integration with other processes; for instance, the cyclic adsorption process through pressure swing adsorption (PSA) has been proven to possess these characteristics. The application of PSA for industrial-grade oxygen production has been proposed and investigated by many researchers since five decades ago and still progressing, implying that the significant advantages of PSA and its continuing development are very demanding. Over the years, various modifications have been introduced to improve the PSA performances for the product purity, recovery, productivity, and energy consumption, in such a way that the penetration of PSA into the market could be amplified and stabilized and make it a cost-sustain alternative technology for oxygen production covering the low to high capacities. The modifications include the engineering design of the PSA itself, such as adding additional steps and material engineering through the adsorbent's modifications.

Symbols

a_p: Specific particle surface per unit volume bed (1/m)
c_i: Gas-phase concentration of component i (kmol/m^3)
C_{pai}: Specific heat capacity of the adsorbed phase (MJ/kmol/K)
C_{ps}: Specific heat capacity of adsorbent (MJ/kmol/K)
C_{pw}: Specific heat capacity of column wall (MJ/kg/K)
C_{vg}: Specific heat capacity of bulk gas-phase (MJ/kmol/K)
$D_{ax,i}$: Axial dispersion coefficient of the component i (m^2/s)

D_B: Bed column diameter (m)
ΔH_i: Heat of adsorption of component i (MJ/kmol)
H_{amb}: Heat transfer coefficient for wall-ambient (MW/m^2/K)
HTC: Heat transfer coefficient for gas-solid phase (MJ/m^2/s)
H_w: Heat transfer coefficient for gas-wall phase (MJ/m^2/s)
k_{ga}: Axial thermal conductivity of bulk gas-phase (MW/m/K)
k_{sa}: Axial thermal conductivity of solid phase (MW/m/K)
k_{LDF}: LDF mass transfer coefficient (1/s)
k_w: Thermal conductivity of column wall (MW/m/K)
M: Molecular weight of bulk gas-phase (kg/kmol)
P: Pressure (bar)
P_H: Adsorption pressure (bar)
P_L: Desorption pressure (bar)
q_i: Solid-phase loading of component i (kmol/kg)
q_i^*: Equilibrium solid-phase loading of component i (kmol/kg)
Re: Reynolds number (-)
r_p: Adsorbent particle radius (m)
t: Time (s)
T: Kelvin (K)
T_0: Reference temperature (K)
T_{amb}: Temperature of ambient (K)
T_g: Temperature of bulk gas-phase (K)
T_s: Temperature of solid-phase (K)
T_w: Temperature of column wall (K)
v_g: Superficial gas velocity (m/s)
W_T: Width of column wall (m)
z: Axial coordinate (m)

Greek letters

ε_i: Interparticle voidage (m^3 void/m^3 bed)
ε_t: Total voidage (m^3 (void + pore)/m^3 bed)
ρ_g: Density of bulk gas-phase (kg/m^3)
ρ_b: Density of adsorbent bulk solid (kg/m^3)
ρ_w: Density of column wall (kg/m^3)
ψ: Adsorbent particle shape factor (-)
μ: Viscosity of bulk gas-phase (kg/m/s)

Abbreviations

AD: Adsorption step
BB: Bed-to-bed
BD: Blowdown step
BTB: Bed-tank-bed
IAST: Ideal adsorbed solution theory
LDF: Linear driving force
LOX: Liquid oxygen system
MSW: Municipal solid waste
OBOGS: On board oxygen generation system
OEC: Oxy-enriched combustion
PE: Pressure equalization step
PR: Pressurization step
PSA: Pressure swing adsorption
PU: Purge step
TPD: Tonne per day
VST: Vacancy solution theory.

Data Availability

The data used to support the findings of the study are included in the text.

Conflicts of Interest

The authors declare that they have no conflicts of interest.

Acknowledgments

The authors want to fully acknowledge the financial support given by Universiti Malaysia Sabah under Skim Dana Khas number SDK0164-2020. The authors thank the GRISM Innovative Solutions for technical support and lastly, the author (M. H. V. Bahrun) is grateful for the financial support from Universiti Teknologi Malaysia.

References

[1] I. Sutton, "Chemicals," in *Plant Design and Operations*, Elsevier, Amsterdam, The Netherlands, 2 edition, 2017.
[2] J.-G. Jee, M.-B. Kim, and C.-H. Lee, "Pressure swing adsorption processes to purify oxygen using a carbon molecular sieve," *Chemical Engineering Science*, vol. 60, pp. 869–882, 2005.
[3] E. J. Shokroo, D. J. Farsani, H. K. Meymandi, and N. Yadollahi, "Comparative study of zeolite 5A and zeolite 13X in air separation by pressure swing adsorption," *Korean Journal of Chemical Engineering*, vol. 33, pp. 1391–1401, 2016.
[4] M. Bałys, E. Brodawka, A. Korzeniewska, J. Szczurowski, and K. Zarębska, "LCA and economic study on the local oxygen supply in Central Europe during the COVID-19 pandemic," *Science of the Total Environment*, vol. 786, Article ID 147401, 2021.
[5] Z. Kamin, M. H. V. Bahrun, and A. Bono, "A short review on pressure swing adsorption (PSA) technology for nitrogen generation from air," *AIP Conference Proceedings*, vol. 2610, Article ID 50006, 2022.
[6] P. Rao and M. Muller, "Industrial oxygen: its generation and use," in *Proceedings of the 2007 ACEEE Summer Study on Energy Efficiency in Industry*, pp. 124–135, Washington, DC, USA, 2007.
[7] M. S. A. Baksh, E. S. Kikkinides, and R. T. Yang, "Lithium type X zeolite as a superior sorbent for air separation," *Separation Science and Technology*, vol. 27, no. 3, pp. 277–294, 1992.
[8] M.-B. Kim, J.-G. Jee, Y.-S. Bae, and C.-H. Lee, "Parametric study of pressure swing adsorption process to purify oxygen using carbon molecular sieve," *Industrial & Engineering Chemistry Research*, vol. 44, no. 18, pp. 7208–7217, 2005.
[9] C. W. Skarstrom, "Method and apparatus for fractionating gaseous mixtures by adsorption," Google, Mountain View, CA, USA, US2944627, 1960.
[10] A. M. M. Mendes, C. A. V. Costa, and A. E. Rodrigues, "Oxygen separation from air by PSA: modelling and experimental results Part I: isothermal operation," *Separation and Purification Technology*, vol. 24, no. 1–2, pp. 173–188, 2001.
[11] D. Ruthven, *Principles of Adsorption and Adsorption Processes*, John Wiley & Sons, New York, NY, USA, 1 edition, 1984.

[12] S. Farooq, D. M. Ruthven, and H. A. Boniface, "Numerical simulation of a pressure swing adsorption oxygen unit," *Chemical Engineering Science*, vol. 44, no. 12, pp. 2809–2816, 1989.

[13] A. Sakoda and M. Suzuki, "The effects of chilled air feed on oxygen-enrichment pressure swing adsorption by simplified computer simulation," *Separations Technology*, vol. 1, no. 2, pp. 73–78, 1991.

[14] M. Xu, H. C. Wu, Y. S. Lin, and S. Deng, "Simulation and optimization of pressure swing adsorption process for high-temperature air separation by perovskite sorbents," *Chemical Engineering Journal*, vol. 354, pp. 62–74, 2018.

[15] C. S. Chang, S. H. Ni, H. S. Yang, and C. T. Chou, "Simulation study of separating oxygen from air by pressure swing adsorption process with semicylindrical adsorber," *Journal of the Taiwan Institute of Chemical Engineers*, vol. 120, pp. 67–76, 2021.

[16] K. S. Knaebel and F. B. Hill, "Pressure swing adsorption: development of an equilibrium theory for gas separations," *Chemical Engineering Science*, vol. 40, no. 12, pp. 2351–2360, 1985.

[17] R. V. Jasra, N. V. Choudary, and S. G. T. Bhat, "Separation of gases by pressure swing adsorption," *Separation Science and Technology*, vol. 26, no. 7, pp. 885–930, 1991.

[18] W. D. Marsh, F. S. Pramuk, R. C. Hoke, and C. W. Skarstrom, "Pressure equalization depressuring in heatless adsorption," Google, Mountain View, CA, USA, US3142547, 1964.

[19] N. H. Berlin, "Method for providing an oxygen-enriched environment," Google, Mountain View, CA, USA, US3280536, 1966.

[20] M. M. Hassan, N. S. Raghavan, and D. M. Ruthven, "Pressure swing air separation on a carbon molecular sieve - II. Investigation of a modified cycle with pressure equalization and no purge," *Chemical Engineering Science*, vol. 42, no. 8, pp. 2037–2043, 1987.

[21] R. T. Yang, *Gas Separation by Adsorption Processes*, Butterworth Publishers, Salem, NH, USA, 1987.

[22] D. M. Ruthven, S. Farooq, and K. S. Knaebel, *Pressure Swing Adsorption*, VCH Publishers, Hoboken, NJ, USA, 1994.

[23] A. S. T. Chiang, "An analytical solution to equilibrium PSA cycles," *Chemical Engineering Science*, vol. 51, no. 2, pp. 207–216, 1996.

[24] S. J. Doong, "An equilibrium model for pressure swing adsorption process with equalization step," in *Fundamentals of Adsorption*, M. D. LeVan, Ed., vol. 356,Springer, Boston, MA, USA, 1996.

[25] H. Shin, "Mathematical simulation of pressure swing adsorption cycle with pressure equalization step," in *Fundamentals of Adsorption*, M. D. LeVan, Ed., vol. 356,Springer, Boston, MA, USA, 1996.

[26] M. Yavary, H. A. Ebrahim, and C. Falamaki, "The effect of number of pressure equalization steps on the performance of pressure swing adsorption process," *Chemical Engineering and Processing: Process Intensification*, vol. 87, pp. 35–44, 2015.

[27] R. Banerjee, K. G. Narayankhedkar, and S. P. Sukhatme, "Exergy analysis of kinetic pressure swing adsorption processes: comparison of different cycle configurations," *Chemical Engineering Science*, vol. 47, no. 5, pp. 1307–1311, 1992.

[28] M. H. Chahbani, R. Talmoudi, A. Abdel Jaoued, and D. Tondeur, "Modeling and simulation of pressure equalization step between a packed bed and an empty tank in pressure swing adsorption cycles," *The Open Chemical Engineering Journal*, vol. 11, pp. 33–52, 2017.

[29] H. Erden and L. Erden, "A simple equalization pressure prediction method for pressure equalization via tanks in PSA process," *International Journal of Scientific and Technological Research*, vol. 4, no. 10, pp. 111–119, 2018.

[30] J. L. Wagner, "Selective adsorption process," Google, Mountain View, CA, USA, US3430418A, 1969.

[31] J. C. Kayser and K. S. Knaebel, "Pressure swing adsorption: experimental study of an equilibrium theory," *Chemical Engineering Science*, vol. 41, no. 11, pp. 2931–2938, 1986.

[32] T. P. Vo, "Repressurization of pressure swing adsorption system," Google, Mountain View, CA, USA, US4376640, 1983.

[33] M. H. V. Bahrun, A. Bono, N. Othman, and M. A. Ahmad Zaini, "Carbon dioxide removal from biogas through pressure swing adsorption - a review," *Chemical Engineering Research and Design*, vol. 183, pp. 285–306, 2022.

[34] AspenTech, *Aspen Adsim Who Should Read This Guide*, Aspen Technology Inc, Loughborough, UK, 2004.

[35] E. Glueckauf, "Theory of chromatography. Part 10: formulae for diffusion into spheres and their application to chromatography," *Transactions of the Faraday Society*, vol. 51, pp. 1540–1551, 1955.

[36] X. Yang, H. Wang, J. Chen et al., "Two-dimensional modeling of pressure swing adsorption (PSA) oxygen generation with radial-flow adsorber," *Applied Sciences*, vol. 9, p. 1153, 2019.

[37] N. D. Hutson, S. U. Rege, and R. T. Yang, "Mixed cation zeolites: Li_xAg_y-X as a superior adsorbent for air separation," *AIChE Journal*, vol. 45, no. 4, pp. 724–734, 1999.

[38] J.-G. Jee, J.-S. Lee, and C.-H. Lee, "Air separation by a small-scaletwo-bed medical O_2 pressure swing adsorption," *Industrial & Engineering Chemistry Research*, vol. 40, no. 16, pp. 3647–3658, 2001.

[39] J.-G. Jee, S.-J. Lee, and C.-H. Lee, "Comparison of the adsorption dynamics of air on zeolite 5A and carbon molecular sieve beds," *Korean Journal of Chemical Engineering*, vol. 21, no. 6, pp. 1183–1192, 2004.

[40] F. E. Epiepang, R. T. Yang, X. Yang, J. Li, and Y. Liu, "Mixed-cationLiCa-lsx zeolite with minimum lithium for air separation," *AIChE Journal*, vol. 64, no. 2, pp. 406–415, 2018.

[41] S. Furmaniak, S. Koter, A. P. Terzyk, P. A. Gauden, P. Kowalczyk, and G. Rychlicki, "New insights into the ideal adsorbed solution theory," *Physical Chemistry Chemical Physics*, vol. 17, no. 11, pp. 7232–7247, 2015.

[42] K. S. Hwang, S. Y. Gong, and W. K. Lee, "Adsorption equilibria for hydrogen and carbon dioxide on activated carbon at high pressure up to 30 atm," *Korean Journal of Chemical Engineering*, vol. 8, no. 3, pp. 148–155, 1991.

[43] M. L. Zanota, N. Heymans, F. Gilles, B. L. Su, M. Frère, and G. De Weireld, "Adsorption isotherms of pure gas and binary mixtures of air compounds on faujasite zeolite adsorbents: effect of compensation cation," *Journal of Chemical and Engineering Data*, vol. 55, no. 1, pp. 448–458, 2010.

[44] S. Suwanayuen and R. P. Danner, "Vacancy solution theory of adsorption from gas mixtures," *AIChE Journal*, vol. 26, no. 1, pp. 76–83, 1980.

[45] C. Béchaud, S. Mélen, D. Lasseux, M. Quintard, and C. H. Bruneau, "Stability analysis of a pressure swing adsorption process," *Chemical Engineering Science*, vol. 56, pp. 3123–3137, 2001.

[46] A. Krauklis, "Modeling of an isothermal pressure swing adsorption process," Stockholm University, Stockholm, Sweden, AEK-NZ-01, 2015.

[47] R. B. Bird, W. E. Stewart, and E. N. Lightfoot, *Transport Phenomena*, John Wiley & Sons, New York, NY, USA, 2nd edition, 2002.

[48] F. P. Incropera and D. P. DeWitt, *Fundamentals of Heat and Mass Transfer*, John Wiley & Sons, New York, NY, USA, 7th edition, 1996.

[49] S. Kumar and S. Jain, "History, introduction, and kinetics of ion exchange materials," *Journal of Chemistry*, vol. 2013, Article ID 957647, 13 pages, 2013.

[50] G. Onyestyák, J. Valyon, and L. V. C. Rees, "The sorption dynamics of N_2 and O_2 in zeolite particles," *Studies in Surface Science and Catalysis*, vol. 158 B, pp. 1019–1026, 2005.

[51] R. T. Yang, *Adsorbents: Fundamentals and Applications*, Wiley-Interscience, Hoboken, NJ, USA, 1st edition, 2003.

[52] Q. Huo, "Synthetic chemistry of the inorganic ordered porous materials," in *Modern Inorganic Synthetic Chemistry*, R. Xu, W. Pang, and Q. Huo, Eds., pp. 339–373, Elsevier B.V, Amsterdam, The Netherlands, 2011.

[53] H. Chen, W. Wang, J. Ding, X. Wei, and J. Lu, "CO_2 adsorption capacity of FAU zeolites in presence of H_2O: a Monte Carlo simulation study," *Energy Procedia*, vol. 105, pp. 4370–4376, 2017.

[54] H. Moradi, H. Azizpour, H. Bahmanyar, N. Rezamandi, and P. Zahedi, "Effect of Si/Al ratio in the faujasite structure on adsorption of methane and nitrogen: a molecular dynamics study," *Chemical Engineering & Technology*, vol. 44, no. 7, pp. 1221–1226, 2021.

[55] S. S. A. Talesh, S. Fatemi, S. J. Hashemi, and M. Ghasemi, "Effect of Si/Al ratio on CO_2 - CH_4 adsorption and selectivity in synthesized SAPO-34," *Separation Science and Technology*, vol. 45, pp. 1295–1301, 2010.

[56] F. Wang, W. Wang, S. Huang, J. Teng, and Z. Xie, "Experiment and modeling of pure and binary adsorption of n-butane and butene-1 on ZSM-5 zeolites with different Si/Al ratios," *Chinese Journal of Chemical Engineering*, vol. 15, no. 3, pp. 376–386, 2007.

[57] A. Zukal, A. Pulido, B. Gil et al., "Experimental and theoretical determination of adsorption heats of CO_2 over alkali metal exchanged ferrierites with different Si/Al ratio," *Physical Chemistry Chemical Physics*, vol. 12, pp. 6413–6422, 2010.

[58] F. E. Epiepang, X. Yang, J. Li, Y. Wei, Y. Liu, and R. T. Yang, "Air separation sorbents: mixed-cation zeolites with minimum lithium and silver," *Chemical Engineering Science*, vol. 198, pp. 43–51, 2019.

[59] R. T. Yang, Y. D. Chen, J. D. Peck, and N. Chen, "Zeolites containing mixed cations for air separation by weak chemisorption-assisted adsorption," *Industrial & Engineering Chemistry Research*, vol. 35, no. 9, pp. 3093–3099, 1996.

[60] A. A. Bhat, H. Mang, S. Rajkumar, T. M. Kotresh, and U. K. Singh, "On-board oxygen generation using high performance molecular sieve," *Defence Life Science Journal*, vol. 2, no. 4, pp. 380–384, 2017.

[61] G. W. Miller, "A 99% purity molecular sieve oxygen generator," in *Proceedings of the Technology 2001: Conference Proceedings: The Second National Technology Transfer Conference and Exposition*, vol. 1, San Jose, CA, USA, December 1991.

[62] J. J. Beaman, "A dynamic model of a pressure swing oxygen generation system," *Journal of Dynamic Systems, Measurement, and Control*, vol. 107, no. 2, pp. 111–116, 1985.

[63] G. W. Miller and C. F. Theis, "Molecular sieve oxygen concentration with secondary oxygen purifier," Google, Mountain View, CA, USA, US4880443, 1999.

[64] Y. Guo, Y. Wang, S. Zhao, and B. Li, "Development and experimental investigation of a multistage oxygen compressor unit with a non-crank mechanism for the onboard oxygen generating system," *Energies*, vol. 13, p. 112, 2020.

[65] R. Sun, T. M. Ismail, X. Ren, and M. Abd El-Salam, "Numerical simulation of gas concentration and dioxin formation for MSW combustion in a fixed bed," *Journal of Environmental Management*, vol. 157, pp. 111–117, 2015.

[66] C. Ma, B. Li, D. Chen et al., "An investigation of an oxygen-enriched combustion of municipal solid waste on flue gas emission and combustion performance at a 8 MWth waste-to-energy plant," *Waste Management*, vol. 96, pp. 47–56, 2019.

[67] M. Lei, C. Sun, and C. Wang, "Techno-economic analysis of a 600MW oxy-enrich pulverized coal-fired boiler," *Energies*, vol. 11, no. 4, 2018.

[68] Z. Riahi, H. Bounaouara, I. Hraiech, M. A. Mergheni, J. C. Sautet, and S. B. Nasrallah, "Combustion with mixed enrichment of oxygen and hydrogen in lean regime," *International Journal of Hydrogen Energy*, vol. 42, no. 13, pp. 8870–8880, 2017.

[69] Z. Zhou, Q. Xue, C. Li, G. Wang, X. She, and J. Wang, "Coal flow and combustion characteristics under oxygen enrichment way of oxygen-coal double lance," *Applied Thermal Engineering*, vol. 123, pp. 1096–1105, 2017.

[70] Z. Fu, S. Zhang, X. Li, J. Shao, K. Wang, and H. Chen, "MSW oxy-enriched incineration technology applied in China: combustion temperature, flue gas loss and economic considerations," *Waste Management*, vol. 38, pp. 149–156, 2015.